Separation Science and Technology
Publication details, including instructions for authors and subscription information:
http://www.informaworld.com/smpp/title~content=t713708471

Simultaneous Absorption of Carbon Dioxide and Sulfur Dioxide into Aqueous 1,8-Diamino-p-menthane

Kyu-Suk Hwang[a]; Dong-Woo Kim[a]; Sang-Wook Park[a]; Dae-Won Park[a]; Kwang-Joong Oh[a]; Seong-Soo Kim[b]
[a] Division of Chemical Engineering, Pusan National University, Busan, Korea [b] Department of Environmental Administration, Catholic University of Pusan, Busan, Korea

Online publication date: 09 December 2009

To cite this Article Hwang, Kyu-Suk , Kim, Dong-Woo , Park, Sang-Wook , Park, Dae-Won , Oh, Kwang-Joong and Kim, Seong-Soo(2009) 'Simultaneous Absorption of Carbon Dioxide and Sulfur Dioxide into Aqueous 1,8-Diamino-p-menthane', Separation Science and Technology, 44: 16, 3888 — 3910
To link to this Article: DOI: 10.1080/01496390903338444
URL: http://dx.doi.org/10.1080/01496390903338444

Separation Science and Technology, 44: 3888–3910, 2009

ISSN: 0149-6395 print/1520-5754 online
DOI: 10.1080/01496390903338444

Simultaneous Absorption of Carbon Dioxide and Sulfur Dioxide into Aqueous 1,8-Diamino-p-menthane

Kyu-Suk Hwang,[1] Dong-Woo Kim,[1] Sang-Wook Park,[1] Dae-Won Park,[1] Kwang-Joong Oh,[1] and Seong-Soo Kim[2]
[1]Division of Chemical Engineering, Pusan National University, Busan, Korea
[2]Department of Environmental Administration, Catholic University of Pusan, Busan, Korea

Abstract: Carbon dioxide and sulfur dioxide were simultaneously absorbed into aqueous 1,8-diamino-p-menthane (DAM) in a stirred semi-batch tank with a planar gas-liquid interface within a range of 0–2.0 kmol/m^3 of DAM, 0.01–0.12 mole fraction of CO_2, 0.001–0.012 mole fraction of SO_2, and 298-318 K. Absorption data of each gas in the CO_2-DAM and SO_2-DAM systems are obtained to verify their reaction regimes, based on film theory, respectively, which are used to analyze the simultaneous absorption mechanisms of CO_2 and SO_2 in the CO_2-SO_2-DAM systems. In the simultaneous absorption rate of CO_2 and SO_2 into DAM solution, the absorption of CO_2 belongs to the second-order reaction of finite rate and the absorption of SO_2 belongs to the instantaneous reaction regime.

Keywords: Carbon dioxide, 1,8-diamino-p-menthane, simultaneous absorption, sulfur dioxide

INTRODUCTION

Carbon dioxide (CO_2) and sulfur dioxide (SO_2) in the flue gas generated from combustion of fossil fuel are the main cause of global, environmental problems such as air pollution and acid rain. The contents of CO_2 and SO_2

Received 17 December 2008; accepted 7 August 2009.
Address correspondence to Sang-Wook Park, Division of Chemical Engineering, Pusan National University, Busan 609-735, Korea. E-mail: swpark@pusan.ac.kr

are 10–15% and 0.1–0.4% in the flue gas from the combustion of fossil fuel such as power plants, respectively. However, the produced volume of flue gas is so large globally that great amounts of CO_2 and SO_2 are introduced into the atmosphere.

Many studies have been done on the mechanisms and kinetics of the reaction of CO_2 with various alkanolamines, employing simple mass balance analysis and resulting in the zwitterion mechanism proposed by Caplow (1) and Danckwerts (2). Some discrepancies remained according to the reaction mechanism (3), particularly the types of amines, gas/liquid contactor, and analysis method used for the rate data, for example, the order of the overall reactions, and the rate constants. Recently, a group of sterically hindered amines were developed (4–6), providing a high capacity of 1.0 mol of CO_2/mol of amine and a relatively high absorption rate, even at high CO_2 loading. A new alkanolamine containing more amines than 1 may be used to provide a high capacity of CO_2/mol of amine.

The absorption of SO_2 into aqueous slurries of sodium, calcium, and magnesium compounds, serving as the absorbent (7–14), and alkaline solutions, has been studied for decades. The medium used in the alkaline solutions was typically alkaline salts (15–19), inorganic acids (20), organic acids (21–24), and amines for reversible reaction (25–29). Danckwerts (30) showed that SO_2 absorption in an alkaline solution is proceeded by an instantaneous reaction while Hikita et al. (31) proposed a penetration theory model based on the two-reaction model using approximate analytical solutions to investigate the kinetics of SO_2 with reactants in the liquid phase.

Gas mixtures containing more than two gases such as NO/SO_2(32) or NO_2/SO_2 (33) emitted from stationary combustion facilities, and H_2S and SO_2 (34,35) from natural, coal, and refinery gases, have been separated by the simultaneous absorption into aqueous slurries or alkaline solutions. Most of these works have been done towards determing the mechanisms and kinetics of the reaction in the simultaneous absorption, proposed by Goetter and Pigford (36) and Hikita et al. (37).

In this present work, CO_2 and SO_2 were absorbed into aqueous 1,8-diamino-p-menthane (DAM) containing functional groups of 2 amines to obtain the reaction kinetics between CO_2 or SO_2 and DAM. To predict the simultaneous absorption rates of CO_2 and SO_2, the film theory equation with the absorption of both the gases was formulated and compared to an approximate solution previously described (6) and the numerical solution. This study, with the absorber of DAM, will make the first attempt for the removal of both the gases emitted from power plant flues and from the viewpoint of energy-efficient separation, and hopefully it will become the preferred treatment over that of conventional, individual separation.

THEORY

The zwitterions mechanism originally proposed by Caplow (1) and later reintroduced by Danckwerts (2) and da Silva and Svendsen (3) is generally accepted as the reaction mechanism in the absorption of CO_2 into aqueous DAM as follows:

$$CO_2 + H_2NRNH_2 = H_2NRN^+H_2COO^- \qquad \text{(i)}$$

$$CO_2 + H_2NRN^+H_2COO^- = O^-OCH_2N^+RN^+H_2COO^- \qquad \text{(ii-1)}$$

$$O^-OCH_2NRN^+H_2COO^- + H_2NRNH_2 = O^-OCHNRNH_2COO^- + H_3N^+RN^+H_3 \qquad \text{(ii-2)}$$

where R presents

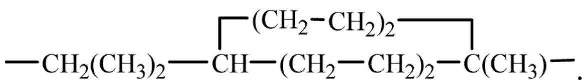

The overall reaction being:

$$CO_2(A) + 2H_2NRNH_2(C) = O^-OCHNRNH_2COO^- + H_3N^+RN^+H_3 \qquad \text{(iii)}$$

The reactions of SO_2 in aqueous DMA, combined with the SO_2 reaction in an aqueous, alkaline solution (15), are as follows:

$$SO_2 + H_2O = 2H^+ + SO_3^{2-} \qquad \text{(iv)}$$

$$H_2NRNH_2 + 2H^+ \rightarrow H_3^+NRNH_3^+ \qquad \text{(v)}$$

The overall reaction being:

$$SO_2(B) + H_2NRNH_2(C) + H_2O \rightarrow 2H_3^+NRNH_3^+ + SO_3^{2-} \qquad \text{(vi)}$$

The irreversible reactions between the dissolved species j and the reactant (C), as shown in reactions (iii) and (vi), may be formulated as follows:

$$j + \nu_j C \rightarrow \text{products} \qquad \text{(vii)}$$

where j is A or B, and ν_j is a stoichiometric coefficients of species j.

The following assumptions are made to set up the mass balance of species j:

1. Henry's law holds,
2. isothermal condition prevails, and
3. species C is a nonvolatile solute,
4. $\nu_A = 1$ and $\nu_B = 1$, and
5. reaction (viii) is mth order with respect to j and nth order with respect to C, of which the reaction rate (r_j) of species j is expressed by:

$$r_j = k_j C_j^m C_C^n \tag{viii}$$

Respective Absorption of CO_2 and SO_2 Accompanied by Reaction in CO_2-DAM and SO_2-DAM System

The mass balances of species A or B and C in CO_2-DAM and SO_2-DAM system using the film theory accompanied by reaction (viii) and the boundary conditions are given as follows:

$$D_j \frac{d^2 C_j}{dz^2} = k_j C_j^m C_C^n \tag{1}$$

$$D_C \frac{d^2 C_C}{dz^2} = \nu_j k_j C_j^m C_C^n \tag{2}$$

$$z = 0; \; C_j = C_{ji}, \frac{dC_C}{dz} = 0 \tag{3}$$

$$z = \delta; \; C_j = 0, C_C = C_{C_o} \tag{4}$$

Depending on the relative rates of diffusion and reaction by using the dimensionless groups listed below, for convenience, the systems may be classified into four regimes: very slow reaction, slow reaction, fast reaction, and instantaneous reaction. The condition for validity of a fast pseudo-mth-order reaction with respect to species j, where the interfacial concentration of species C is the same as that in the bulk liquid phase, is given by the following expression (38):

$$3 < Ha << E_i \tag{5}$$

where

$$Ha = \frac{\sqrt{\frac{2}{m+1} D_j k_j C_{ji}^{m-1} C_{Co}^n}}{k_{Lj}} \text{ and } E_i = 1 + \frac{C_{Co}}{\nu_j C_{ji}} \frac{D_C}{D_j} \tag{6}$$

Under the condition of Eq. (5), Eq. (1) can be written as:

$$D_j \frac{d^2 C_j}{dz^2} = k_j C_j^m C_{Co}^n = k_m C_j^m \tag{7}$$

where

$$k_m = k_j C_{Co}^n \tag{8}$$

Using the analytical solution of Eq. (7) with the boundary conditions of Eq. (3) and (4), N_A at the interface is:

$$N_j = C_{ji} \sqrt{\frac{2}{m+1} D_j k_j C_{ji}^{m-1} C_{Co}^n} \tag{9}$$

Where the resistance in the gas phase was not negligible, the expression for N_j for the pseudo-mth order reaction regime was derived as follows:

$$\frac{P_j}{N_j} = \frac{1}{k_G} + \frac{H_j}{\sqrt{\frac{2}{m+1} D_j k_j C_{ji}^{m-1} C_{Co}^n}} \tag{10}$$

According to Eq. (10), Plots of P_j/N_j vs. $H_j/(D_j k_j C_{Co})^{0.5}$ at m=n=1 should be a straight line with slope of 1.

Simultaneous Absorption of Both Gases CO_2 and SO_2 into Reactive DAM Solution

For simultaneous absorption of both CO_2(A) and SO_2(B) into aqueous DAM (C) solution, the following assumptions (6) are made to set up the mass balance of species j and C:

1. The presence of one gas does not affect the rate of absorption of the other gas because the gases do not compete for the common liquid-phase reactant C,
2. the reaction orders with respect to A and B are 1 and 1, respectively.

The mass balances of species j and C using the film theory accompanied by chemical reaction and the boundary conditions are given as follows:

$$D_j \frac{d^2 C_j}{dz^2} = k_j C_j C_C \tag{11}$$

$$D_C \frac{d^2 C_C}{dz^2} = \sum_{j=A}^{B} \nu_j k_j C_j C_C \tag{12}$$

$$z = 0;\ C_j = C_{ji};\ \frac{dC_C}{dz} = 0 \tag{13}$$

$$z = \delta;\ C_j = 0,\ C_C = C_{Co} \tag{14}$$

The flux of species j at the interface of the gas-liquid phase is defined by

$$N_j = -D_j \left(\frac{dC_j}{dz}\right)_{z=0} \tag{15}$$

The enhancement factor (β) here is defined as the ratio of molar flux of Eq. (5) with the chemical reaction to that obtained without chemical reaction:

$$\beta_j = -\frac{N_j}{k_{L_j} C_{ji}}\bigg|_{Z=0} \tag{16}$$

The solution of Eqs. (11) and (12) is used to obtain the value of β_j through Eq. (16).

The total absorption rate (N_T) for the simultaneous absorption of CO_2 and SO_2 is obtained using β_j and physical absorption rate of species j (N_{jo}) as follows:

$$N_T = \sum_{j=A}^{B} \beta_j N_{jo} \tag{17}$$

Simultaneous Absorption of Both Gases CO_2 of Second Reaction and SO_2 of Instantaneous Reaction into Reactive DAM Solution

If the reaction between CO_2 and DAM of Eq. (iii) is assumed to be a second-order reaction of finite rate and the reaction between SO_2 and DAM of Eq. (vi) to be an instantaneous reaction, the reaction of SO_2 and DAM occurs at a reaction plane (λ), where the concentration of both SO_2 and DAM are zero. CO_2 diffuses beyond the reaction plane and reacts with C in the region between the reaction plane and the bulk liquid.

The mass balance describing the diffusion of A, B, and C in the liquid film, based on film theory, is as follows:

$0 < z < \lambda$,

$$D_A \frac{d^2 C_A}{dz^2} = 0 \tag{18}$$

$$D_B \frac{d^2 C_B}{dz^2} = 0 \tag{19}$$

$\lambda < z < \delta$,

$$D_A \frac{d^2 C_A}{dz^2} = k_A C_A C_C \tag{20}$$

$$D_C \frac{d^2 C_C}{dz^2} = \nu_A k_A C_A C_C \tag{21}$$

The boundary conditions are:

$$z = 0 : C_A = C_{Ai}, C_B = C_{Bi} \tag{22}$$

$$z = \lambda : C_A = C_A^*, C_B = 0, C_C = 0 \tag{23}$$

$$-\nu_B D_B (dC_B/dz) = D_C (dC_C/dz) \tag{24}$$

$$z = \delta : C_A = 0, C_C = C_{Co} \tag{25}$$

Eqs. (20) and (21) are nonlinear and cannot be solved analytically.

However, Hikita et al. (37) have presented an approximate analytical solution with the enhancement factors (β_A and β_B) of species A and B absorbing two gases, one of which reacts instantaneously in the liquid phase, as follows:

$$\beta_A = \frac{[1 + r_B q_B + r_C q_C) - (1 + r_B q_B)\beta_A]\gamma\eta}{(1 + r_C q_C - \beta_A)\tanh(\gamma\eta)} \tag{26}$$

where,

$$\eta = \frac{1 + r_C q_C - \beta_A}{1 + r_B q_B + r_C q_C - \beta_A} \sqrt{\frac{1 + r_B q_B + r_C q_C - (1 + r_B q_B)\beta_A}{3 r_C q_C \beta_A}}$$

$$\beta_B = \frac{1 + r_B q_B + r_C q_C - \beta_A}{r_B q_B} \tag{27}$$

where,

$$r_B = \frac{D_B}{D_A}, r_C = \frac{D_C}{D_A}, q_B = \frac{\nu_B C_{Bi}}{\nu_A C_{Ai}}, q_C = \frac{C_{Co}}{\nu_A C_{Ai}}, \gamma = \frac{\sqrt{k_A C_{Co} D_A}}{k_L}$$

β_A and β_B are obtained from Eqs. (26) and (27) by a trial and error procedure with given, dimensionless parameters such as r_B, r_C, q_B, q_C, and γ.

EXPERIMENTAL

Chemicals

All chemicals were of reagent grade, and used without further purification. Purity of CO_2, N_2, SO_2 were more than 99.9%. CO_2, N_2, and SO_2 were supplied by Hanna Gas Company, Korea, and 1,8-diamino-p-menthane by Aldrich Chemical Company, U.S.A.

Absorption Rate of CO_2 and SO_2

Absorption experiments were carried out in an agitated vessel (6,39). The absorption vessel was constructed of glass with an inside diameter of 0.073 m and a height of 0.151 m. Four, equally spaced vertical baffles, each one-tenth of the vessel diameter in width, were attached to the internal wall of the vessel. The gas and liquid phase were agitated with an agitator driven by a 1/4 Hp variable speed motor. A straight impeller 0.034 m in length and 0.05 m in width was used as the liquid phase agitator and located at the middle position of the liquid phase. The surface area was calculated as a ratio of the volume of added water to the measured height of water in the absorber, and its value was 40.947 cm^2. The gas and liquid in the vessel were agitated at a speed of 50 rpm. The value of the cumulative volume of the soup bubble was measured by a soup bubbler for the change of absorption time to obtain the absorption rate of CO_2 and SO_2. Each experiment was duplicated at least once under identical conditions. It was assumed that the volumetric rising rate of the soup bubble in the soup bubbler attached to the absorption vessel was equal to the value of the absorption rate of gases. The gaseous compositions of CO_2 and SO_2 at inlet of the absorber were using gas chromatography (column: PTFE, 6 feet $\times$ 1/8 inch OD, Chromosorb 107, 80/100; Detector: TCD). The absorption experiments were carried out in a range of 0–2.0 kmol/m^3 of DAM, 0.01–0.12 mole fraction of CO_2, 0.001–0.012 of SO_2, and 298–318 K at atmospheric pressure.

A sketch of the experimental set up is presented in Fig. 1. A typical experimental run was carried out as follows (6): The vent valve A is initially closed and the purge value B is open. Gas is flowed continuously through the absorber D, so as to make sure that the latter is filled with gas at the start of the experiment. During this initial period, the water bath temperature is brought up to the desired value, and the liquid batch is kept in bottle F inside the water bath. At the start of the experiment, the liquid batch is poured into funnel G and the agitator E in D is started. The liquid feed valve C is closed, the purge value B is closed, and the vent valve A is opened, as simultaneously as possible. Measurements are started at the soap film meter H taking care that there are always two soap films in the meter so that a continuous reading of the cumulative volume of gas which has flowed through the soap film meter (V) can be recorded as a function of time. The gas absorption rate was obtained as a slope of the plots of V vs. time at an initial time. The molar flux of species j (N_j) was calculated by the following equation with the initial volumetric absorption rates of CO_2, $V(t_1)/t_1$, obtained from the cumulative volume of gas which has flowed through the soap film meter.

$$N_j = \frac{P_T - P_W^o}{SRT} \frac{V(t_1)}{t_1} \tag{28}$$

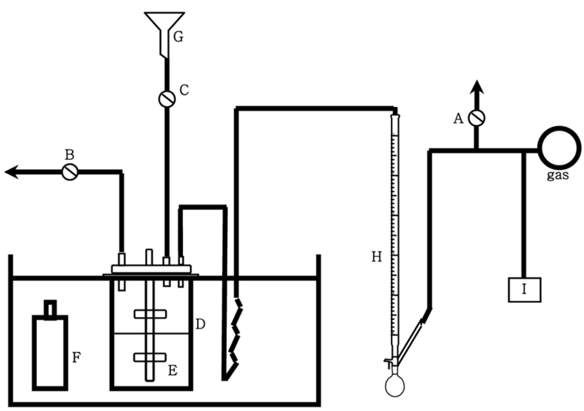

A, B, C : Valve
D : Absorber
E : Impeller
F : Liquid bottle
G : Funnel
H : Soap film meter
I : Gas chromatography

Figure 1. Schematic diagram of the agitated vessel.

where P_T is the atmospheric pressure, P_W^o, the vapor pressure of water, S, the surface area of liquid phase, V(t_1), the cumulative volume of gas during the absorption time, t_1.

Physicochemical Properties

Both the solubility and diffusivity of solute gases in the liquid medium to solve the differential equations of Eqs. (1), (2), (11), and (12) are obtained as follows:

The Henry constant of CO_2 in water is obtained from the empirical equations (40):

$$H_A^o = 2.8249 \times 10^6 \exp\left(-\frac{2044}{T}\right) \tag{29}$$

The Henry constant of SO_2 in water was estimated by the empirical formula (41):

$$H_B^o = 101.3/\exp\left(\frac{510}{T_o} - 26970T_1 + 155T_2 - 0.0175T_oT_3/R\right) \tag{30}$$

where, $T_o = 298.15, T_l = l/T_o - l/T.T_3 = T_3 = T_o/T - l + \ln(T/T_o)$, $T_3 = T/T_o - T_o/T - 2\ln(T/T_o)$

The solubility (C_{ji}) of species j at a given partial pressure (P_j) in aqueous solution of a given concentration of DAM was estimated as follows:

$$P_j = H_j^o C_{ji} \tag{31}$$

The diffusivity of CO_2 in water is obtained from the empirical equations (40):

$$D_A^o = 2.35 \times 10^{-6} \exp\left(-\frac{2119}{T}\right) \tag{32}$$

The diffusivity of SO_2 in water was estimated by the empirical formula (42):

$$D_B^o = 5.08982 \times 10^{-12} T \exp\left(5.15581 - \frac{1243.06}{T - 53.19}\right) \tag{33}$$

The diffusivity of species j in aqueous DAM solution (43) was estimated as follows:

$$D_j = D_j^o \left(\frac{\mu_w}{\mu}\right)^{2/3} \tag{34}$$

D_C was estimated by the method of Wilke (30).

Viscosity of aqueous DAM solution was measured using a Brookfield viscometer (Brookfield Eng. Lab. Inc, USA).

RESULTS AND DISCUSSION

Absorption of CO_2 in CO_2-DAM System

To determine the reaction order with respect to CO_2 and DAM in a fast reaction regime of CO_2-DAM system, the absorption rates ($N_{A,exp}$) of CO_2 were measured in a range of 0–2.0 kmol/m^3 of DAM, 0.01–0.12 mole fraction of CO_2, and 298–318 K.

Figure 2 shows logarithmic plots of $N_{A,exp}$ vs. C_{Ai} at a typical C_{Co} of 0.1 kmol/m^3 and different temperatures.

The plots present straight lines (correlation coefficient (r^2) > 0.999) with a slope of unity in each temperature. This, according to Eq. (9), indicates that the reaction order with respect to CO_2 is 1.

To determine the reaction order with respect to the concentration of DAM, logarithmic plots of $N_{A,exp}/C_{Ai}D_A^{0.5}$ vs. C_{Co} at a typical y_A of 0.02 and different temperatures are shown in Fig. 3.

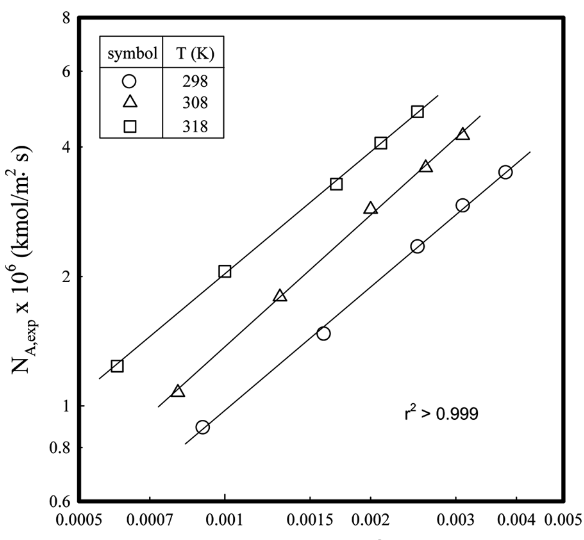

Figure 2. Effect of C_{Ai} on N_A into aqueous DAM at $C_{Co} = 0.1$ kmol/m^3 and different temperatures.

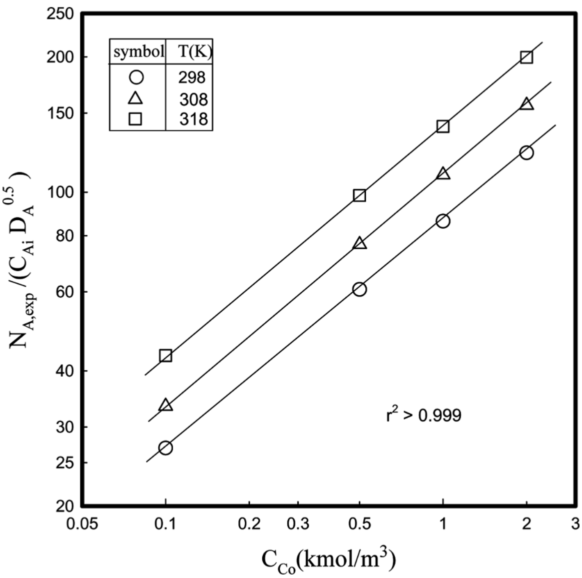

Figure 3. Determination of reaction rate constant (k_A) and order with respect to DAM at $y_A = 0.02$ and different temperatures.

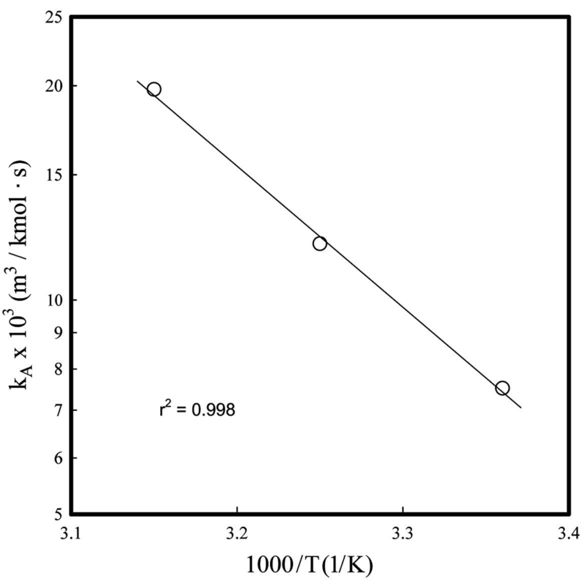

Figure 4. Arrhenius plot of the CO_2-DAM system.

Each of these plots as shown in Fig. 3 is a straight line ($r^2 > 0.999$) with a slope of 1. This, according to Eq. (9), indicates that the reaction order with respect to DAM is 1.

The values of the reaction rate constant (k_A) of CO_2-DAM were calculated from the intercept of the plots of data in Fig. 3 and they have been found to be 7516, 11998, 19766 m^3/kmol·s at 298, 308, 318 K, respectively. Figure 4 shows the Arrhenius plots of the values of k_A at different temperatures using data mentioned above.

Linear regression analysis of the Arrhenius plots gives the following expression for k_A ($r^2 = 0.998$).

$$k_A = 1.72 \times 10^{12} \exp(-5747/T) \tag{41}$$

Table 1. The values of H_a and E_i in CO_2/DAM and SO_2/DAM system

T(K)	C_{Co}(kmol/m^3)	y_A	Ha	E_i	T(K)	C_{Co}(kmol/m^3)	y_B	Ha	E_i
298	0.1	0.01	159	189	298	0.1	0.001	29	32
		0.02	76	95			0.002	14	16
		0.04	39	48			0.004	7	9
		0.08	21	25			0.008	4	5
		0.12	11	17			0.012	3	4
308	0.1	0.01	184	239	308	0.1	0.001	43	44
		0.02	103	120			0.002	19	23
		0.04	45	60			0.004	10	12
		0.08	21	31			0.008	5	6
		0.12	13	21			0.012	4	5
318	0.1	0.01	219	295	318	0.1	0.001	59	61
		0.02	122	148			0.002	28	31
		0.04	72	75			0.004	14	16
		0.08	26	38			0.008	7	8
		0.12	19	26			0.012	4	6
298	0.1	0.02	76	95	298	0.1	0.002	14	16
	0.5		179	471		0.5		33	77
	1.0		264	942		1.0		48	153
	2.0		399	1882		2.0		73	306
308	0.1	0.02	102	120	308	0.1	0.02	19	23
	0.5		239	595		0.5		45	110
	1.0		350	1189		1.0		66	218
	2.0		521	2378		2.0		98	435
318	0.1	0.02	122	148	318	0.1	0.02	29	31
	0.5		282	736		0.5		66	148
	1.0		412	1470		1.0		97	296
	2.0		611	2939		2.0		143	590

The corresponding value of the activation energy has been calculated to be 48.0 kJ/mol.

To validate the condition of a fast pseudo-first-order reaction with respect to CO_2, the values of Ha and E_i were calculated and listed in Table 1. Because the values of Ha and E_i in Table 1 satisfy Eq. (5), the absorption of CO_2 into DAM solution in this study belongs to a fast reaction regime.

To ensure that the gas phase resistance is really negligible in all run, plots of $P_A/N_{A,exp}$ vs. $H_A^o/(k_A D_A C_{Co})^{0.5}$ at different temperatures have been made following Eq. (10) for m = 1, n = 1. These plots are presented in Fig. 5.

It can be seen from Fig. 5 that all plots of $P_A/N_{A,exp}$ vs. $H_A^o/(k_A D_A C_{Co})^{0.5}$ are straight lines with slope of 1, passing through the origin with $r^2 = 0.991$. This, according to Eq. (10), signifies negligible gas phase resistance.

The specific rate ($N_{A,fem}$) of CO_2 absorption was estimated from the solution of Eqs. (1) and (2) with the boundary conditions of Eqs. (3) and (4), using the numerical method of FEMLAB program. The comparison of the observed and estimated molar flux of CO_2 in DAM concentration range of 0.1–2.0 kmol/m^3, 0.02 mole fraction of CO_2, and 298–313 K is shown in Fig. 6.

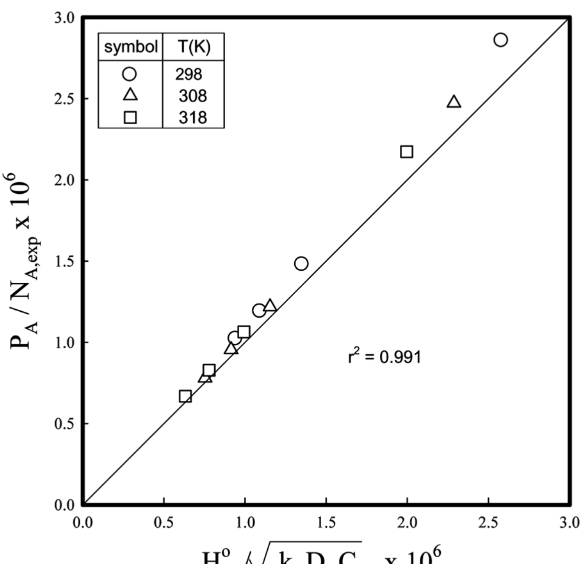

Figure 5. Verification of no gas phase resistance for absorption of CO_2 into aqueous DAM at $y_A = 0.02$ and different C_{CO} and temperatures.

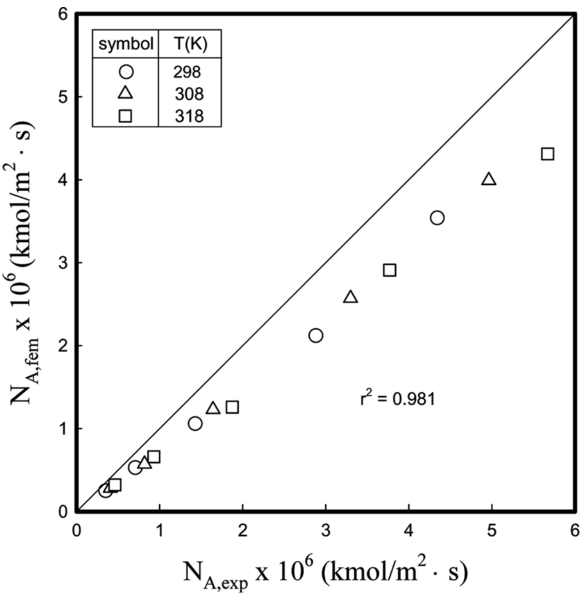

Figure 6. Comparison of estimated and measured values of absorption rate of CO_2.

As shown in Fig. 6, the observed values of the molar flux agree with the estimated values ($r^2 = 0.981$) and standard deviation $= 0.038$), suggesting that the governing equation of Eqs. (1) and (2), as well as the estimated physical properties such as C_{Ai}, D_A, and D_C, may be plausible.

Absorption of SO_2 in SO_2-DAM System

To determine the reaction order with respect to the concentration of SO_2 and DAM in SO_2-DAM system, the absorption rates ($N_{B,exp}$) of SO_2 were measured with a range of 0–2.0 kmol/m^3 of DAM, 0.001–0.012 mole fraction of SO_2, and 298–318 K.

To determine the reaction order with respect to SO_2, logarithmic plots of $N_{B,exp}$ vs. C_{Bi} at a typical C_{Co} of 0.1 kmol/m^3 and different temperatures are shown in Fig. 7.

The plots present straight lines ($r^2 > 0.987$) with a slope of unity in each temperature. This, according to Eq. (9), indicates that the reaction order with respect to SO_2 is 1.

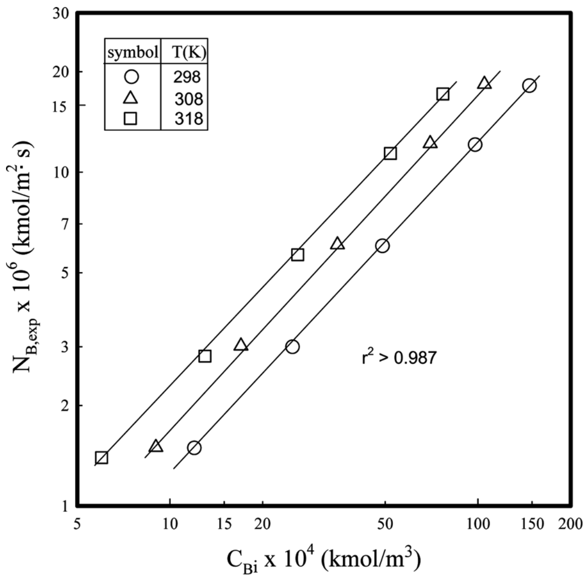

Figure 7. Effect of C_{Bi} on N_B into aqueous DAM at $C_{Co} = 0.1\,\text{kmol/m}^3$ and different temperatures.

To determine the reaction order with respect to the concentration of DAM, logarithmic plots of $N_{B,exp}/C_{Bi}D_B^{0.5}$ vs. C_{Co} at a typical y_B of 0.002 are shown in Fig. 8.

Each of these plots as shown in Fig. 8 is a straight line ($r^2 > 0.985$) with a slope of 1. This, according to Eq. (9), indicates that the reaction order with respect to DAM is 1.

The values of the reaction rate constant (k_B) of SO_2-DAM were calculated from the intercept of the plots of data in Fig. 8 and they have been found to be 12076, 19265, 29224 m^3/kmol·s at 298, 308, 318 K, respectively. Figure 9 shows the Arrhenius plots of the values of k_B at different temperatures using data mentioned above.

Linear regression analysis of the Arrhenius plots gives the following expression for k_B ($r^2 = 0.991$).

$$k_B = 6.43 \times 10^{11} \exp(-5309/T) \tag{42}$$

The corresponding value of the activation energy has been calculated to be 44.2 kJ/mol.

To validate the condition of a fast pseudo-first-order reaction with respect to SO_2, the values of Ha and E_i were calculated and listed in Table 1. Because the values of Ha and E_i in Table 1 satisfy Eq. (5), the

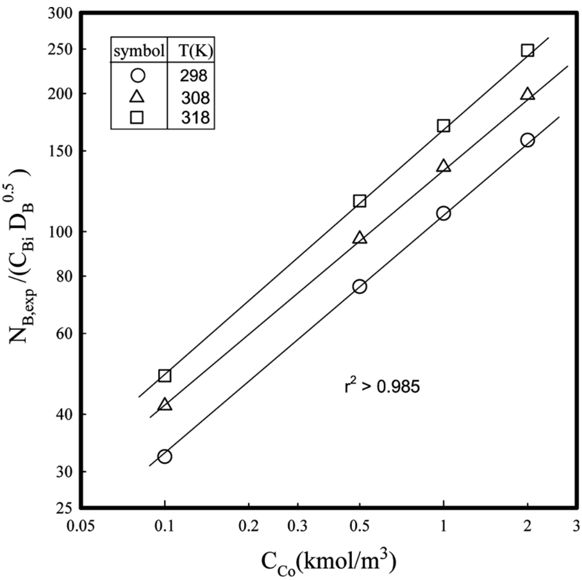

Figure 8. Determination of reaction rate constant (k_B) and order with respect to DAM at $y_A = 0.002$ and different temperatures.

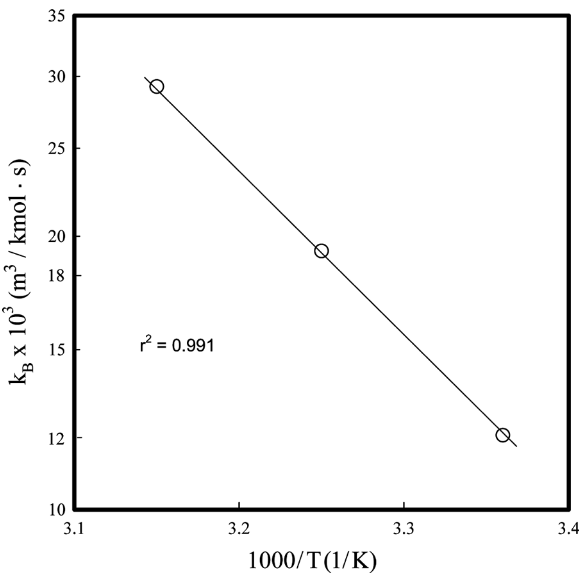

Figure 9. Arrhenius plot of the SO_2-DAM system.

absorption of SO_2 into DAM solution in this study belongs to a fast reaction regime.

To ensure that the gas phase resistance is really negligible in all run, plots of $P_B/N_{B,exp}$ vs. $H_B^o/(k_B D_B C_{Co})^{0.5}$ at different temperatures have been made following Eq. (10) for m = 1, n = 1. These plots are presented in Fig. 10.

It can be seen from Fig. 10 that all plots of $P_B/N_{B,exp}$ vs. $H_B^o/(k_B D_B C_{Co})^{0.5}$ are straight lines with slope of 1, passing through the origin with $r^2 = 0.993$. This, according to Eq. (10), signifies negligible gas phase resistance.

The specific rate ($N_{B,fem}$) of SO_2 absorption was estimated from the solution of Eq. (1) and (2) with the boundary conditions of Eq. (3) and (4), using the numerical method of FEMLAB program. The comparison of the observed and estimated molar flux of SO_2 in DAM concentration range of 0.1–2.0 kmol/m^3, 0.002 mole fraction of CO_2, and 298–313 K is shown in Fig. 11.

As shown in Fig. 11, the observed values of the molar flux agree with the estimated values ($r^2 = 0.988$ and standard deviation = 0.011), suggesting that the governing equation of Eqs. (1) and (2), as well as the estimated physical properties such as C_{Bi}, D_B, and D_C, may be plausible.

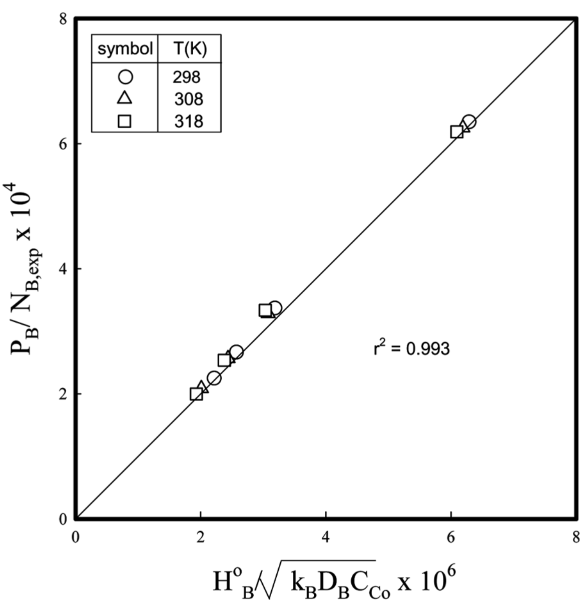

Figure 10. Verification of no gas phase resistance for absorption of SO_2 into aqueous DAM at $y_A = 0.002$ and different C_{CO} and temperatures.

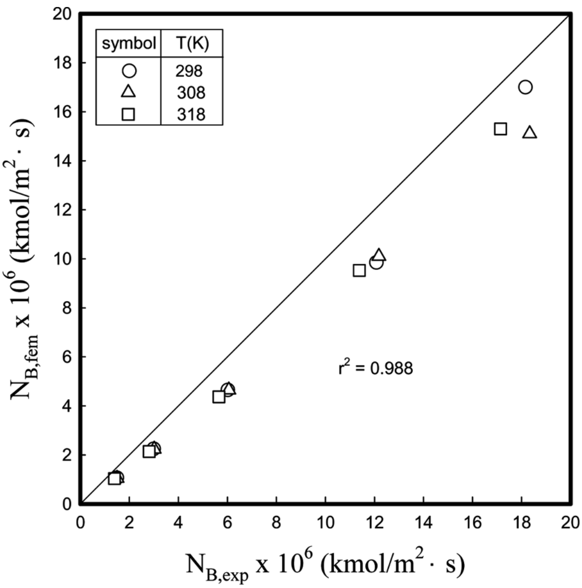

Figure 11. Comparison of estimated and measured values of absorption rate of SO_2.

The diffusivity (D_A and D_B) and solubility (C_{Ai} and C_{Bi}), required to solve the differential equations of Eqs. (1) and (2), are affected by the physical properties of the solution and the calculated fluxes ($N_{A,fem}$ and $N_{B,fem}$) increase with decreasing them. D_A and D_B were corrected with the viscosity of the solution using Eq. (34), but C_{Ai} and C_{Bi} in water were used. Because C_{Ai} and C_{Bi} might be larger than them in the DAM solution, $N_{A,fem}$ and $N_{B,fem}$ were smaller than $N_{A,exp}$ and $N_{B,exp}$, as shown in Figs. 6 and 11.

Simultaneous Absorption of CO_2 and SO_2 in CO_2-SO_2-DAM System

Mixtures of gases of CO_2 and SO_2 are simultaneously absorbed into aqueous DAM solution within a range of 0.1–2.0 kmol/m^3 of DAM at 0.2 mole fraction of CO_2, 0.02 mole fraction of SO_2, and 298 K to obtain the simultaneous absorption rate (N_T).

The experimental absorption rate ($N_{T,exp}$) was plotted against C_{Co} in Fig. 12.

As shown in Fig. 12, $N_{T,exp}$ increases with increasing C_{Co}, due to increase in concentrations of the reactant of DAM.

The simultaneous absorption rate ($N_{T,fem}$) of CO_2 and SO_2 was obtained from the solution of Eqs. (11) and (12) with the boundary

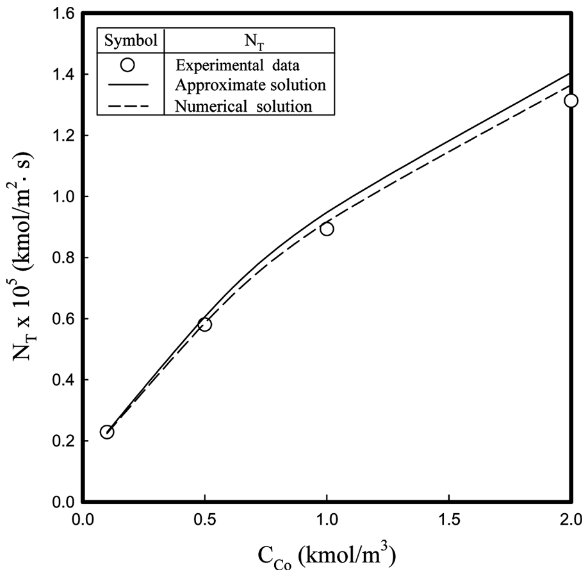

Figure 12. Simultaneous absorption rate of CO_2 and SO_2 at $y_A = 0.2$ and $y_B = 0.02$, and 25°C.

conditions of Eqs. (13) and (14), using the numerical method of FEMLAB program and plotted as dotted line in Fig. 12. On the other hand, it ($N_{T,ins}$) was obtained by Eq. (17) through β_A and β_B of Eqs. (26) and (27) under the conditions of the fast reaction regime in CO_2-DAM system and the instantaneous reaction regime in SO_2-DAM system and as the solid line in Fig. 12. As shown in Fig. 12, $N_{T,exp}$ approaches to $N_{T,fem}$ more closely with correlation coefficient (r^2) of 0.995 than $N_{T,ins}$ with r^2 of 0.983 and $N_{T,ins}$ approaches to $N_{T,fem}$ very well with r^2 of 0.996. This means that the approximate analytical solution, presented by Hikita et al. (37), under the conditions that the absorption of CO_2 belongs to the second-order reaction of finite rate and the absorption of SO_2 belongs to the instantaneous reaction regime may be used to predict the simultaneous absorption rate of CO_2 and SO_2 into DAM solution.

CONCLUSIONS

Mixture of CO_2 and SO_2 are simultaneously absorbed into DAM in a stirred, semi-batch tank with a planar, gas-liquid interface within a range of 0–2.0 $kmol/m^3$ of DAM, 0.01–0.12 mole fraction of CO_2, 0.001–0.012 mole fraction of SO_2, and 298–318 K. Diffusivity and Henry constants of CO_2 and SO_2 were obtained from the reference data.

Absorption data of CO_2 and SO_2 in DAM solution are used to verify that the reactions in CO_2-DAM system and SO_2-DAM are first order with respect to both gases and DAM. The measured rates of simultaneous absorption of CO_2 and SO_2 were compared with those calculated by the numerical and approximate solutions of mass balances with reaction regimes of both gases through verification of the reaction regime in the CO_2-SO_2-DAM system.

ACKNOWLEDGMENTS

This work was supported by Brain Korea 21 Project and a grant (2006-C-CD-11-P-03-0-000-2007) from the Energy Technology R&D of Korea Energy Management Corporation. Dae-Won Park is also thankful for KOSEF (R01-2007-000-10183-0).

REFERENCES

1. Caplow, M. (1968) Kinetics of carbamate formation and breakdown. *J. Am. Chem. Soc.*, *90*: 6795.
2. Danckwerts, P.V. (1979) The reaction of CO_2 in ethanolamines. *Chem. Eng. Sci.*, *34*: 443.
3. da Silva, E.F.; Sendsen, H.F. (2004) Ab initio study of the reaction of caramate formation from CO_2 and alkanolamine. *Ind. Eng. Chem. Res.*, *43*: 3413.
4. Mimura, T.; Suda, T.; Honda, A.; Kumazawa, H. (1998) Kinetics of reaction between carbon dioxide and sterically hindered amines for carbon dioxide recovery from power plant flue gases. *Chem. Eng. Commun.*, *170*: 245.
5. Park, S.W.; Park, D.W.; Oh, K.J. (2008) Absorption of carbon dioxide into aqueous solution of sodium glycinate. *Sep. Sci. Technol.*, *43*: 3003.
6. Park, S.W.; Park, D.W.; Oh, K.J.; Kim, S.S. (2009) Simultaneous absorption of carbon dioxide and sulfur dioxide into aqueous 2-amino-2-methyl-1-propanol. *Sep. Sci. Technol.*, *44*: 543.
7. Sada, E.; Kumazawa, H.; Nishimura, H. (1983) Absorption of sulfur dioxide into aqueous double slurries dontaining limestone and magnesium hydroxide. *AIChE J.*, *29*: 60.
8. Uchida, S.; Ariga, O. (1985) Absorption of sulfur dioxide into limestone slurry in a stirred tank. *Can. J. Chem. Eng.*, *63*: 778.
9. Egan, B.Z.; Felker, L.K. (1986) Removal of SO_2 from simulated flue gas by magnesia spray absorption. *Ind. Eng. Chem. Process Des. Dev.*, *25*: 558.
10. Ruhland, F.; Kind, R.; Weiss, S. (1991) The kinetics of the absorption of sulfur dioxide in calcium hydroxide suspensions. *Chem. Eng. Sci.*, *46*: 939.

11. Brogren, C.; Karlsson, H.T. (1997) Modeling the absorption of SO_2 in a spray scrubbing using the penetration theory. *Chem. Eng. Sci.*, *52*: 3085.
12. Berman, Y.; Tanklevsky, A.; Oren, Y.; Tamir, A. (2000) Modeling and experimental studies of SO_2 absorption in coaxial cylinders with impinging streams: Part I. *Chem. Eng. Sci.*, *55*: 1009.
13. Stein, J.; Kind, M.; Schlunder, E. (2002) The influence of HCl on SO_2 absorption in the spray dry scrubbing process. *Chem. Eng. J.*, *86*: 17.
14. Hikita, H.; Asai, S.; Nose, H. (1978) Absorption of sulfur dioxide into water. *AIChE J.*, *24*: 147–149.
15. Hikita, H.; Asai, S.; Tsufi, T. (1977) Absorption of sulfur dioxide into aqueous solution sodium hydroxide and sodium sulfite solution. *AIChE J.*, *23*: 538.
16. Roberts, D.L.; Friedlander, S.K. (1980) Sulfur dioxide transport through aqueous solutions: Part I. Theory. *AIChE J.*, *26*: 593.
17. Chang, C.S.; Rochelle, G.T. (1981) SO_2 absorption into aqueous solution. *AIChE J.*, *27*: 292.
18. Hikita, H.; Konish, K. (1983) The absorption of SO_2 into aqueous Na_2CO_3 solutions accompanied by the desorption of CO_2. *Chem. Eng. J.*, *27*: 167.
19. Ebrahimi, S.; Picioreanu, C.; Kleerebezem, R.; Heijnen, J.J.; van Loosdrecht, M.C.M. (2003) Rate-based modeling of SO_2 absorption into aqueous $NaHCO_3/Na_2CO_3$ solutions accompanied by the desorption of CO_2. *Chem. Eng. Sci.*, *58*: 3589.
20. Colle, S.; Vanerschuren, J.; Thomas, D. (2004) Pilot-scale validation of the kinetics of SO_2 absorption into sulfuric acid solutions containing hydrogen peroxide. *Chem. Eng. Process*, *43*: 1397.
21. Erga, O. (1986) SO_2 recovery by means of adipic acid buffers. *Ind. Eng. Chem. Fundam.*, *25*: 692.
22. Regalbuto, M.C.; Strieder, W.; Varma, A. (1991) An extension of semi-empirical gas-liquid equilibrium model for sulfur dioxide absorption in aqueous sodium citrate solution. *Chem. Eng. Sci.*, *46*: 3314.
23. Xia, J.; Rumpf, B.; Maurer, G. (1999) Solubility of sulfur dioxide in aqueous-solutions of acetic acid, sodium acetate, and ammonium acetate in the temperature range from 313 to 393 K at pressures up to 3.3 MPa. *Ind. Eng. Chem. Res.*, *38*: 1149.
24. Dutta, B.K.; Basu, R.K.; Pandit, A.; Ray, P. (1987) Absorption of SO_2 in citric acid-solution citrate buffer solutions. *Ind. Eng. Chem. Res.*, *26*: 1291–1296.
25. Ho, M.P.; Klinzing, G.E. (1986) Absorption of sulfur dioxide and nitric oxide by amines and N-cyclohexyl-2-pyrrolidone. *Can J. Chem. Eng.*, *64*: 243.
26. Riesenfeld, F.C.; Kohl, A.L. (1974) *Gas Purification*; Gulf Publ. Co.: Houston.
27. Basu, R.K.; Dutta, B.K. (1987) Kinetics of absorption of sulfur dioxide in dimethylaniline solution. *Can. J. Chem. Eng.*, *65*: 27.
28. van Dam, M.H.H.; Lamine, A.S.; Roizard, D.; Lochon, P.; Roizard, P. (1997) Selective sulfur dioxide absorption using organic solvents. *Ind. Eng. Chem. Res.*, *36*: 4628–4637.

29. Nagel, D.; de Kermadec, R.; Lintz, H.G.; Roizard, C.; Lapicque, F. (2002) Absorption of sulfur dioxide in *N*-formylmorpholine: Investigations of the kinetics of the liquid phase reaction. *Chem. Eng. Sci.*, *57*: 4883.
30. Danckwerts, P.V. (1970) *Gas-Liquid Reactions*; McGraw-Hill: New York.
31. Hikita, H.; Asai, S.; Takatsuka, T. (1972) Gas absorption with a two step instantaneous chemical reaction. *Chem. Eng. J.*, *4*: 31.
32. Ho, M.P.; Klinzing, G.E. (1986) Absorption of sulfur dioxide and nitric oxide by amines and N-cyclohexyl-2-pyrrolidone. *Can J. Chem. Eng.*, *64*: 243.
33. Sada, E.; Kumazawa, H.; Yoshikawa, Y. (1988) Simultaneous removal of NO and SO_2 by absorption into aqueous mixed solutions. *AIChE J.*, *34*: 1215.
34. Hix, R.M.; Lynn, S. (1991) Reactive absorption of H_2S by a solution of SO_2 in poly (glycol ether): Effect of a volatile dissolved reactant on mass transfer enhancement. *Ind. Eng. Chem. Res.*, *30*: 930.
35. Kenig, E.Y.; Schneider, R.; Gorak, A. (1999) Rigorous dynamic modeling of complex reactive absorption processes. *Chem. Eng. Sci.*, *54*: 5195.
36. Goetter, L.A.; Pigford, R.L. (1971) Computational studies of the simultaneous chemical absorption of two gases. *AIChE J.*, *17*: 793.
37. Hikita, H.; Asai, S.; Ishikawa, H. (1979) Simultaneous absorption of two gases in a reactive liquid, one gas reacting instantaneously. *Chem. Eng., J.*, *18*: 169.
38. Daraiswany, L.K.; Sharma, M.M. (1984) *Heterogeneous Reaction: Analysis, Example and Reactor Design*; John Wiley Sons: New York.
39. Yu, W.; Astarita, G.; Savage, D.W. (1985) *Chem. Eng. Sci.*, *40*: 1585.
40. Versteeg, G.F.; van Swaaij, W.P.M. (1988) Solubility and diffusivity of acids gases (CO_2, N_2O) in aqueous alkanolamine solutions. *J. Chem. Eng. Data*, *33*: 29.
41. Saha, A.K.; Bandyopadhyay, S.S.; Biswas, A.K. (1993) Solubility and diffusivity of N_2O and CO_2 in aqueous solutions of 2-amino-methyl-1-propanol. *J. Chem. Eng. Data*, *38*: 78.
42. Pasiuk-Bronikowska, W.; Rudzinski, K.J. (1991) Absorption of SO_2 into aqueous systems. *Chem. Eng. Sci.*, *46*: 2281.
43. Cussler, E.L. (1984) *Diffusion*; Cambridge University Press: New York.